Decay spectroscopy of element 115 daughters: ^{280}Rg → ^{276}Mt and ^{276}Mt → ^{272}Bh

J. M. Gates,[1,*] K. E. Gregorich,[1] O. R. Gothe,[1,2] E. C. Uribe,[1,2] G. K. Pang,[1] D. L. Bleuel,[3] M. Block,[4] R. M. Clark,[1]
C. M. Campbell,[1] H. L. Crawford,[1] M. Cromaz,[1] A. Di Nitto,[5] Ch. E. Düllmann,[4,5,6] N. E. Esker,[1,2] C. Fahlander,[7] P. Fallon,[1]
R. M. Farjadi,[1] U. Forsberg,[7] J. Khuyagbaatar,[4,6] W. Loveland,[8] A. O. Macchiavelli,[1] E. M. May,[1,2] P. R. Mudder,[1,2]
D. T. Olive,[1,2] A. C. Rice,[1,2] J. Rissanen,[1] D. Rudolph,[7] L. G. Sarmiento,[7] J. A. Shusterman,[1,2] M. A. Stoyer,[3] A. Wiens,[1]
A. Yakushev,[4] and H. Nitsche[1,2]

[1]*Lawrence Berkeley National Laboratory, Berkeley, California 94720, USA*
[2]*University of California, Berkeley, California 94720, USA*
[3]*Lawrence Livermore National Laboratory, Livermore, California 94551, USA*
[4]*GSI Helmholtzzentrum für Schwerionenforschung GmbH, 64291 Darmstadt, Germany*
[5]*Johannes Gutenberg-Universität Mainz, 55099 Mainz, Germany*
[6]*Helmholtz Institute Mainz, 55099 Mainz, Germany*
[7]*Lund University, 22100 Lund, Sweden*
[8]*Oregon State University, Corvallis, Oregon 97331, USA*

Forty-six decay chains, assigned to the decay of ^{288}115, were produced using the ^{243}Am(^{48}Ca,3n)^{288}115
reaction at the Lawrence Berkeley National Laboratory 88-in. cyclotron. The resulting series of α decays were
studied using α-photon and α-x-ray spectroscopies. Multiple α-photon coincidences were observed in the element
115 decay chain members, particularly in the third- and fourth-generation decays (presumed to be ^{280}Rg and ^{276}Mt,
respectively). Upon combining these data with those from 22 ^{288}115 decay chains observed in a similar experiment,
updated level schemes in ^{276}Mt and ^{272}Bh (populated by the α decay of ^{280}Rg and ^{276}Mt, respectively) are proposed.
Photons were observed in the energy range expected for K x rays coincident with the α decay of both ^{280}Rg and
^{276}Mt. However, Compton scattering of higher-energy γ rays and discrete transitions are present in the K x-ray
region preventing a definitive Z identification to be made based on observation of characteristic K x-ray energies.
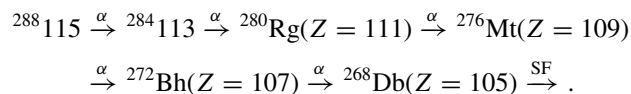
Over the past 15 years, a collaboration working at the Flerov
Laboratory for Nuclear Reactions (FLNR) has reported the
discovery of six new superheavy elements (SHEs) assigned
atomic numbers $Z = 113$–118 and more than 50 new iso-
topes using reactions of ^{48}Ca beams with actinide targets
[1–3]. Since 2007, experiments conducted at Lawrence Berke-
ley National Laboratory (LBNL) [4,5], the GSI Helmholtzzen-
trum für Schwerionenforschung (GSI) [6–11], and FLNR [12]
have confirmed the production and decay properties for the
majority of isotopes produced in ^{48}Ca + actinide reactions.
However, although decay properties are well understood, a
decade old question remains: Can atomic numbers of SHEs
be confirmed? Nature has not been kind—the SHE isotopes
discovered in recent years decay through a series of α
decays that terminate in spontaneous fission (SF) without
passing through previously known nuclides. With no decay
connection to nuclides for which mass numbers A and Z are
firmly established, assignments for these new SHE isotopes
are based primarily on measurement of excitation functions,
cross bombardments, and α-decay systematics. Therefore,
assignments ultimately rely on mass models. However, one
method to firmly establish Z is through the observation of
characteristic K x rays, the energies of which have been
accurately and precisely calculated [13–15]; this method has
been previously used to identify $Z > 100$ [16] and is a
promising avenue in the case of SHEs.

The nuclides assigned to SHEs are presumed to form in
complete-fusion–neutron-evaporation reactions with excep-
tionally low cross sections. Beam intensities of $>10^{12}$ particles
per second are required to form SHEs at the rate of only
atoms per day or week. Therefore, spectroscopic information
has historically been limited to α-particle energies. However,
in the past few years, detailed spectroscopy of the heaviest
elements has been investigated using in-beam isomer and
decay spectroscopies [17]. In the latter, electromagnetic nu-
clear transitions are detected in coincidence with the α decay.
The highly selective α trigger in this method provides nearly
background-free photon spectra, allowing for investigation of
the nuclear structure of levels above the ground state in the
daughter nucleus, even in the challenging case of the SHEs [9].
Such coincidence measurements may provide a path toward
identifying characteristic K x rays, thus establishing Z for the
heaviest elements.

Recent papers [9,18] report on results of decay spectroscopy
performed at GSI for isotopes populated along decay chains
presumed to originate from the ^{243}Am(^{48}Ca,3n)^{288}115 reac-
tion. For brevity, such wording will hereafter be eliminated,
and all Z and A assignments are presumed. Decay chains
assigned to ^{288}115 typically proceed through a series of
α decays to ^{268}Db where the chain terminates in SF as
follows:

$$^{288}115 \xrightarrow{\alpha} {}^{284}113 \xrightarrow{\alpha} {}^{280}\text{Rg}(Z = 111) \xrightarrow{\alpha} {}^{276}\text{Mt}(Z = 109)$$

$$\xrightarrow{\alpha} {}^{272}\text{Bh}(Z = 107) \xrightarrow{\alpha} {}^{268}\text{Db}(Z = 105) \xrightarrow{\text{SF}} .$$

*jmgates@lbl.gov

Of interest in Ref. [9] are the first candidates for K x rays, assigned in the decay step $^{276}\text{Mt} \rightarrow {}^{272}\text{Bh}$. We report here on the higher statistics results of experiments performed at LBNL, similarly aimed at the spectroscopy of element 115 (E115) and its daughters, produced in the bombardment of ^{48}Ca on ^{243}Am.

Beams of $^{48}\text{Ca}^{11+}$ were produced from enriched metallic Ca in the VENUS ion source and accelerated through the LBNL 88-in. cyclotron to laboratory energies of 262 MeV. After passing through a differential pumping section that serves to separate the vacuum of the beamline from the 53-Pa helium fill gas inside the Berkeley gas-filled separator (BGS) [19], the beam was delivered to the BGS. Immediately downstream of the differential pumping section, the beam was incident on a rotating ($\sim$10-Hz) target consisting of four arc-shaped $^{243}\text{Am}_2\text{O}_3$ targets, prepared by electrodeposition of ^{243}Am onto 2.7(1)-μm-thick titanium backings. Two target wheels were used during the irradiations with an initial average ^{243}Am thickness of 540(35) $\mu\text{g/cm}^2$.

Typical on-target ^{48}Ca beam intensities were one-particle microampere. Energy losses through target matter were calculated using SRIM2012 [20]. The resulting center-of-target laboratory-frame beam energy was 242(2) MeV, corresponding to an excitation energy of 36(2) MeV. The E115 compound nucleus evaporation residues (EVRs) were formed with the momentum of the beam and recoiled out of the target and into the fill gas of the BGS. In the BGS, the EVRs were separated from the beam and unwanted reaction products based on differing magnetic rigidities ($B\rho$) in He gas. $B\rho$'s of the E115 EVRs were estimated as described in Ref. [19], and the BGS magnets were adjusted to center the E115 EVRs on the BGS focal plane, resulting in a $B\rho = 2.275$ T m.

Detection and identification of E115 decay chain members was performed using the corner-cube-clover (C3) focal plane detector. The C3 detector consists of silicon-strip detectors surrounded by high-purity germanium clover-type detectors. Following flight through the BGS, E115 EVRs were implanted into one of three 32×32 strip double-sided silicon-strip detectors (DSSDs), each with an active area of 64×64 mm^2. These are arranged to form the corner of a cube and sit inside of a three-sided pyramidal vacuum chamber with 2-mm-thick aluminum walls, positioned such that the apex projects outward along the beam axis. A hexagonal array of trapezoidal single-sided silicon-strip detectors (SSSDs) was installed directly upstream of the implantation detectors. Spontaneous fission fragments or α particles that recoil out of the face of the DSSDs can implant into another DSSD or SSSD where their full energy can be recovered by summing recorded energies. α particle energies determined this way are referred to as reconstructed energies. Full energy α-particle detection efficiency was measured to be 77(5)% based on data from the $^{208}\text{Pb}(^{48}\text{Ca},2n)\,^{254}\text{No}$ reaction. The remaining α particles (referred to as escape events) escape the face of the DSSD, without further interaction, depositing only a fraction of their energy in the DSSD. One clover detector is placed directly against each face of the pyramid, immediately behind each DSSD. The efficiency for detecting photons emitted from a particle implanted in the DSSD was estimated using a mixed γ-ray calibration source positioned to simulate several sites in the DSSD and verified experimentally with

the $^{207}\text{Pb}(^{48}\text{Ca},2n)\,^{253}\text{No}$ reaction. The photon efficiency is maximum at 30(2)% for $E_{ph} = 120$ keV. Efficiency is well reproduced in GEANT4 simulations of the C3 setup [21] where the simulated photopeak efficiency of $E_{ph} = 120$ keV originating from implanted activity was 31%.

Data acquisition was triggered by an event in one of the DSSDs or SSSDs with an energy above $\sim$500 keV during beam or $\sim$200 keV when the beam was shut off. One σ-α particle resolution was 20 keV for events with their full energy in the DSSD and 50–160-keV for reconstructed energies. The average photon energy resolution was 2 keV below 1 MeV.

During the first part of the experiment, a multiwire proportional counter (MWPC) was placed $\sim$20 cm upstream of the C3 detector to differentiate events originating in the C3 detector (decays) from those passing through the separator and implanting. During the second part of the experiment, the MWPC was removed to increase the implantation depth of the EVRs, thus increasing the recorded energy of escape events.

A two-stage fast beam shutoff was employed to reduce background in the search for decay chains from E115. When the MWPC was in place, a first-stage 30-s beam shutoff was initiated upon detection of an EVR [$5 < E(\text{MeV}) < 18$, coincident with the MWPC] followed within 30 s by an α-like particle [$8.8 < E(\text{MeV}) < 11$, anticoincident with the MWPC]. When the MWPC was removed, the beam was shut off for 30 s following the detection of an EVR [$8 < E(\text{MeV}) < 17$] followed within 15 s by an α-like particle [$8.8 < E(\text{MeV}) < 11$]. If a second α-like particle was observed during the first-stage shutoff, a 60-s second-stage shutoff was initiated. There were 2024 stage-one and 35 stage-two beam shutoffs during the measurement. All 35 stage-two beam shutoffs were associated with an identified E115 chain.

The average rates of photon, EVR-, α-, escape-, and SF-like events in the C3 detector are summarized in Table I. A two-dimensional silicon germanium timing gate was used that contained over 95% of the prompt coincidences. The gate was 240-ns wide at 500 keV and 360-ns wide at 120 keV.

During analysis, decay chains originating from E115 were identified using correlations that consisted of: (a) an EVR followed by two or more α-like events within 20 s, or (b) an EVR followed by one or more α-like events and a SF [$E(\text{MeV}) > 100$] within 20 s. We expect 0.2 and 0.003 random chains of these types, respectively. While establishing the E115 decay chains, there were several cases where candidate chains had missing members and/or more escapelike events than expected, arising from the nonzero probability that:

TABLE I. Average rates of photon-, EVR-, α-, and escapelike events in the C3 detector while the beam was on target and during beam shutoffs.

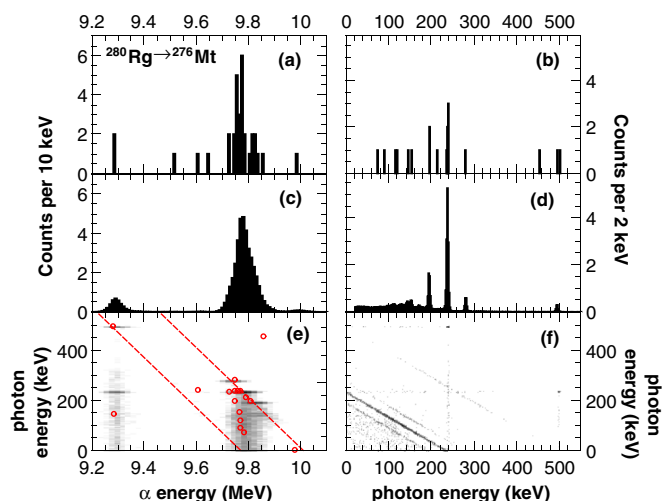| 1	Beam on (Hz/pixel)	Beam off (Hz/pixel)
EVR	2.3×10^{-4}	0
α	8.5×10^{-5}	4.4×10^{-6}
Escape	0.07	0.01
SF	1.1×10^{-6}	6.2×10^{-7}
Photon	21 kHz/crystal	1.7 kHz/crystal

FIG. 1. (Color online) (a) Combined spectrum of α particles (no reconstructed values) observed in the LBNL experiment and Ref. [9] for the decay step ^{280}Rg $\rightarrow$ ^{276}Mt. (b) Combined photon spectrum observed in the LBNL experiment and Ref. [9]. (c) GEANT4 simulations of expected α-particle spectrum assuming the level scheme in Fig. 2(a). (d) GEANT4 simulations of the expected photon spectrum assuming the level scheme in Fig. 2(a). (e) α-photon matrix from observed coincidences in the LBNL experiment and Ref. [9] (circles) superimposed on GEANT4 simulations of expected α-photon coincidences. The dashed lines represent $E_\alpha + E_{ph} = 10\,000$ and 9760 keV. (f) GEANT4 simulations of expected photon-photon coincidences. In (e) and (f), the gray scale darkens with the logarithm of counts.

(i) an escaping α particle deposited energy below the trigger threshold in the DSSD, or (ii) a random α- or escapelike event is observed within the decay chains. In these cases, ambiguous assignments were evaluated statistically. The likelihoods for various interpretations of assignments along a chain were calculated based on known lifetimes, α-decay energies (from

Refs. [9,22] the LBNL experiment), and the available energy and correlation time data. The results of these analyses are included in the Supplemental Material [23].

Forty-six decay chains from the decay of 115, were observed and are included in the Supplemental Material [23]. All of these chains were assigned to ^{288}115 based on comparison with the decay properties in Refs. [9,22,24]. Two α-photon coincidences were observed between the α decays attributed to ^{288}115, ^{284}113, and ^{272}Bh. This is consistent with the expected sum of 2.1 random α-photon coincidences expected in the ^{288}115, ^{284}113, and ^{272}Bh spectra. Twenty-eight α-photon (-photon) coincidences were observed with the decays of ^{280}Rg (14 α-photon coincidences) and ^{276}Mt (2 α-photon-photon and 12 α-photon coincidences) in the LBNL experiment. We expect 0.2 and 0.2 random photonlike events below 1 MeV to be correlated to real α or escape events from the decays of ^{280}Rg and ^{276}Mt, respectively. Additionally, if a random event has been mistakenly assigned as a real α or escape event, then an additional 0.001 and 0.6 random photonlike events, respectively, are expected for each incorrect assignment.

Combining data from the LBNL experiment and Ref. [9], 20 photons were observed in coincidence with α decays attributed to ^{280}Rg. The experimental α and photon spectra are presented in Figs. 1(a) and 1(b). Six photons with an average energy of 237.4(5) keV were observed coincident with α particles with $E_{\alpha-avg}$(MeV) $= 9.77(1)$. This supports the assignment of a 237(1)-keV level populated by a 9.77(1)-MeV α decay as in Fig. 3 of Ref. [9] and a Q_α(MeV) $= 10.15(1)$ with a maximum allowed $E_{\alpha\text{-}max}$ (MeV) $= 10.01(1)$. We have included this in the level scheme in Fig. 2(a) as a firmly established level in ^{280}Rg.

The data from the LBNL experiment also contain indications of decays from ^{280}Rg to additional states in the ^{276}Mt daughter. A small peak in the α spectrum appears at 9.28(1) MeV, and one α-photon coincidence between a 9.28(2)-MeV α particle and a 494.2(13)-keV photon was observed. The sum energy of $E_\alpha + E_{ph}$(MeV) $= 9.77(2)$ and suggests an excited state at 732 keV decaying to the 237-keV level. We have

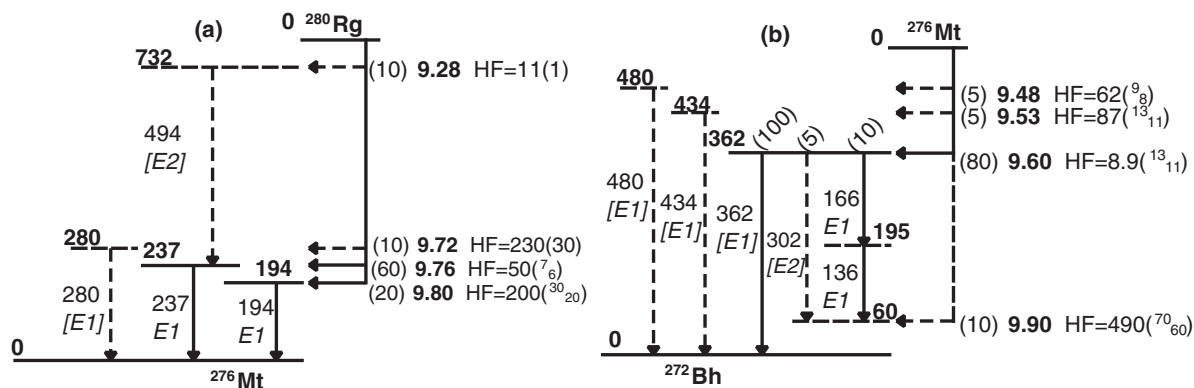FIG. 2. Proposed level schemes for the decay of (a) ^{280}Rg $\rightarrow$ ^{276}Mt and (b) ^{276}Mt $\rightarrow$ ^{272}Bh. Firmly established levels and transition energies are solid lines, and tentative levels and transition energies are dashed lines. Bold numbers represent energy of a given level, numbers in parentheses are relative α-decay populations of a given level or photon intensity from that level. Labels to the left of the vertical arrows indicate the energy and multipolarity of a given transition. Multipolarities that were not experimentally determined and, therefore, assumed for purposes of generating the simulated spectra, are in square brackets. Derived hindrance factors HF $= T_{1/2}^{exp}/T_{1/2}^{sys}$, where experimental half-lives of ^{280}Rg and ^{276}Mt were calculated to be $4.1(^{5}_{4})s$ and $0.63(^{9}_{7})s$, respectively, using data from the LBNL experiment and Refs. [9,22] and $T_{1/2}^{sys}$ was calculated according to Ref. [28].

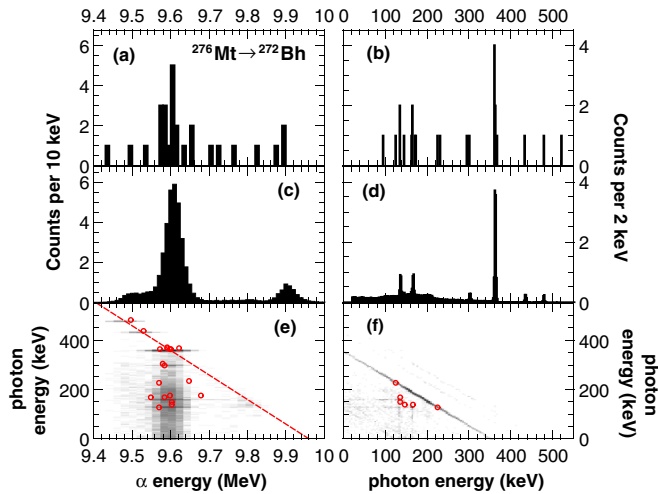FIG. 3. (Color online) The same as Fig. 1, expect it is for the decay step ^{276}Mt $\rightarrow$ ^{272}Bh, using the level scheme in Fig. 2(b), and the dashed line in (e) represents $E_\alpha + E_{ph} = 9960$ keV.

tentatively included it in the level scheme in Fig. 2(a). Unlike in Ref. [9], no 194-keV photons were observed in the LBNL experiment. However, a peak in the experimental α spectrum was observed at E_α(MeV) = 9.82(1) and $E_\alpha + E_{ph}$(MeV) = 10.01(1), consistent with $E_{\alpha\text{-max}}$ calculated above. GEANT4 simulations show that this is more likely due to a 9.81-MeV α particle feeding a level 194 keV above the ground state than the arrangement discussed in Ref. [9]; the former has been included in Fig. 2(a). A coincidence in the LBNL experiment was observed between a 279.6(22)-keV photon and a 9.75(2)-MeV α particle. $E_\alpha + E_{ph}$(MeV) = 10.03(2) is within 1σ of the $E_{\alpha\text{-max}}$, indicating another excited state, tentatively included in Fig. 2(a).

Three additional photons were observed in coincidence with ^{280}Rg α particles and deserve discussion: A 452.7(25)-keV photon was observed in coincidence with a 9.86(2)-MeV α. The sum of $E_\alpha + E_{ph}$(MeV) = 10.31(2) and is larger than the $E_{\alpha\text{-max}}$ determined above. This may indicate a random coincidence or that the full energy of the decay is not included in the current level scheme, i.e., that all transitions in Fig. 2(a) decay to a long-lived (relative to our coincidence window) state $\sim$300 keV above the ground state. We have adopted the random photon explanation. One escape event was observed in coincidence with a 1075.9(26) photon and may indicate another high-lying transition or a random photon. Another escape event was observed in coincidence with a 498.9(27)-keV photon. This may originate from the same level as the previously discussed 494.2(13)-keV photon.

To establish limits on expectations for Compton scattering, transition multipolarities, relative population of states, etc., within the proposed decay schemes, we have used realistic GEANT4 [25,26] simulations of the experimental setup [21] to simulate E115 α-decay chains assuming the proposed level schemes. One hundred thousand simulated ions were implanted into a virtual C3 detector and allowed to decay. The energy and time of hits in each C3 detector element were recorded and sent through analysis codes used for experimental

data. During postprocessing, events were randomly chosen to have either C3 or TASISpec resolution according to the relative size of the two data sets. New α-particle and photon energies were chosen from Gaussian distributions to reproduce the characteristic C3 and TASISpec resolutions. To compare with experimental data, spectra obtained from simulations were normalized using a common normalization factor.

Using the combined data from the LBNL experiment and Ref. [9] along with GEANT4 simulations, we can assign transition multipolarities to the most intense transitions. Conversion coefficients taken from Ref. [27] for a $M1$, $E1$, or $E2$ transition in $Z = 109$ near 200 keV are approximately 9, 0.09, and 1.5, respectively. If the 237-keV transition were $M1$, we would expect to observe 9.4 K x rays per 237-keV photon. If the transition were $E2$, then $\alpha + e^-$ summing in converted transitions would result in 1.8 events with energies above 9.9 MeV in the DSSD spectrum for every observed 237-keV photon. Only the assignment of $E1$ to the 237-keV transition as suggested in Ref. [9] where we expect 0.11 K x rays and 0.2 events above 9.9 MeV in the α spectrum per observed 237-keV photon agrees with the observed spectra. A similar argument can be used to determine the most likely multipolarity of the 194-keV transition. Only the assignment of $E1$ to the 194-keV transition as suggested in Ref. [9] where we expect 0.13 K x rays and 0.2 events above 9.9 MeV in the α spectrum per observed 194-keV photon is consistent with the data.

For the rest of the transitions, the data were insufficient to assign transition multipolarities. For the purpose of simulations, they were assumed to be the multipolarities shown in Fig. 2(a). The GEANT4 simulations of α and photon spectra assuming the proposed ^{280}Rg $\rightarrow$ ^{276}Mt level scheme are shown in Figs. 1(c) and 1(d), respectively. In Figs. 1(e) and 1(f), the simulated α-photon and photon-photon coincidence spectra, respectively, are shown in comparison to the observed events. There is good agreement between the GEANT4 simulations and the experimental data. The simulations indicate that the combined data set should include (7×237)-, (3×194)-, (2×280)-, and (0.4×494)-keV photons, in good agreement with the observed 6, 2, 1, and 1, respectively. An additional ten Compton events and 0.7 K x rays are expected. This compares well to the eight photons below 490 keV that were not assigned to specific transitions.

We now turn our attention to the question of Z identification along this step of the decay chain. In the absence of background in the K x-ray region (i.e., from Compton events, discrete transitions, or random photons), the observation of three or more $K\alpha$ x rays is required for a statistically significant Z identification. In the case of the ^{280}Rg $\rightarrow$ ^{276}Mt decay step, transitions above the K-shell edge are expected to contribute two Compton events to the K x-ray region. Without the ability to distinguish between Compton events and K x rays, Z identification is more complicated and requires observation of a characteristic K x-ray spectrum, which we are defining as: (i) Intensity $I_{K\alpha1} \geqslant I_{K\alpha2}$ and $I_{K\alpha} \gg I_{K\beta}$ and (ii) one of the $K\alpha$ peaks more than 2σ above background.

Two photons in the LBNL experiment [see Fig. 1(b)] were observed with $E_{ph} = 152.1(24)$ and 144.5(25) keV. These energies are within 1σ of the expected energies

of Mt ($Z = 109$) $K\alpha$ x rays where $E_{K\alpha2}(\text{keV}) = 142.69$, $E_{K\alpha1}(\text{keV}) = 151.89$, $E_{K\beta135}(\text{keV}) = 169.81$, and $E_{K\beta24}(\text{keV}) = 175.46$ [13]. Internal conversion of the transitions in the level scheme presented in Fig. 2(b) should lead to the observation of 0.7 K x rays, according to the GEANT4 simulations. However, these simulations, which reproduce the experimental α and photon spectra well [see Figs. 1(c) and 1(d)], indicate that 2.6 Compton photons are expected in the K x-ray region from 140 to 180 keV. Although one or both of the observed photons may be Mt K x rays, they cannot be distinguished from the Compton background. Z identification is not possible in the decay step $^{280}\text{Rg} \rightarrow {}^{276}\text{Mt}$ with the current summed data set. We generated multiple photon spectra using GEANT4 and assuming the production of 10^2–10^4 E115 decay chains. Simulation of 3000 chains was required before the observation of a characteristic x-ray spectrum (as defined above) was observed in 50% of the spectra simulated for the decay step $^{280}\text{Rg} \rightarrow {}^{276}\text{Mt}$ (i.e., 60 times the statistics obtained in the combined data sets).

The combined data sets from the LBNL experiment and Ref. [9] contain 50 α decays, attributed to ^{276}Mt. A plot of the α and photon spectra from the combined data set is shown in Figs. 3(a) and 3(b). There were seven photons averaging 362.2(5) keV. Six of these photons were coincident with α particles with an average energy of 9.60(1) MeV. This supports the assignment of a 9.60(1)-MeV α decay populating a level 362 keV above the ground state as in the level scheme proposed in Fig. 3 of Ref. [9], which results in a maximum $E_{\alpha\text{-max}} = 9.96(1)$ MeV and $Q_\alpha = 10.10(1)$ MeV.

Several photons were also observed above 362 keV, namely, at $E_{\text{ph}}(\text{keV}) = 434(1)$, 479.6(23), and 522.3(14). These were in coincidence with α particles of 9.53(1), 9.50(2) MeV, and an escape, respectively. These coincidences are intriguing and may indicate decays to states above the 362-keV transition. In the case of the 434- and 479.6-keV photons, the sums of $E_\alpha + E_{\text{ph}}$ are 9.96(1) and 9.98(2) MeV, respectively, within 1σ of $E_{\alpha\text{-max}} = 9.96(1)$ MeV. However, these transitions are not further supported by peaks in the α-particle spectrum and are tentatively included in the level scheme presented in Fig. 2(b).

In this experiment and Ref. [9], three photon-photon coincidences were observed with the α decay of ^{276}Mt with photon energies of 136(1)/167(1), 135.7(26)/147.0(20), and 126.6(12)/227.0(25) keV. The latter was coincident with a 9.57(2)-MeV α, and the sum of the two photon energies is within 3σ of 362 keV. The coincidence is likely a 362-keV photon that Compton scattered between two of the unshielded Ge crystals. The other two coincidences contain photons within 2σ of expected $Z = 107$ K x-ray energies ($E_{K\alpha2}(\text{keV}) = 136.19$, $E_{K\alpha1}(\text{keV}) = 144.48$, $E_{K\beta135}(\text{keV}) = 162.90$, and $E_{K\beta24}(\text{keV}) = 167.12$ [13]) and warrant further discussion. We first turn our attention to the 167(1)-keV photon: Two additional photons of 164.4(26) and 165.7(22) keV were observed in the LBNL experiment, coincident with α particles of 9.58(2) and 9.55(5) MeV, respectively. Although these photons are within 1σ of expected $K\beta24$ x-ray energies, the $K\beta24$ doublet is expected to contribute <5% to the total K x-ray spectrum. Therefore, the presence of three 166(1)-keV photons indicates a discrete transition. Based on the observed

α-particle energies, the 166(1)-keV transition likely originates from the 362-keV level. Now we move our attention to the 137(1)- and 135.7(26)-keV photons and whether these may be K x rays: The 135.7(26)-keV photon was observed in coincidence with a 9.60(2)-MeV α. Additionally, the sum of 136(1) and 167(1) is 303(1) keV, and a 302(1)-keV photon was observed in Ref. [9], coincident with a 9.58(1)-MeV α. Combined, these data are consistent with a cascade of nonconverted transitions from the 362-keV level to a 60(1)-keV level, proceeding through either a 196- or a 226-keV level. A tentative cascade has been added to the level scheme assuming the former. To interpret the 147.0(20)/135.7(26) coincidence, we note that with two low-energy γ-γ coincidences, we expect one of the four photons to be a Compton event. The 147-keV photon is consistent with energy expected from Compton scattering of a 166-keV photon in the material between the DSSD and the Ge detectors. Further evidence of this 60(1)-keV state is contained in the α spectrum. The endpoint of the α spectrum occurs at 80(10)-keV below $E_{\alpha\text{-max}}$ but within 2σ of the 60(1)-keV level, indicating that the highest-energy α decay populates the low-lying level and not the ground state.

The data can be used to determine the multipolarity of the 166- and 136-keV transitions. $M1$ and $E2$ conversion coefficients for transitions around 130–160 keV are > 5, whereas $E1$ conversion coefficients are < 0.1. The number of observed γ rays of 166 and 136 keV as well as the observation of γ-γ coincidences can only be accounted for if the γ-γ cascade is composed of two $E1$ transitions. Figure 3 includes GEANT4 simulations of this level scheme along with the experimental data for comparison. Simulations indicate that we should have observed (5×362)-, (2×166)-, (3×136)-, (0.7×303)-, (0.4×434)-, and (0.3×478)-keV photons, which is in good agreement with the observed 7, 3, 2, 1, 1, and 1, respectively. Simulations also indicate that we should have ten Compton-scattered photons in the spectrum, which compares well with the eight photons that were not assigned to discrete transitions.

We again turn our attention to the question of Z identification along this decay step in the chain: $^{276}\text{Mt} \rightarrow {}^{272}\text{Bh}$. This step is particularly interesting as possible observation of K x-ray candidates was previously put forward in Ref. [9]. The combined photon spectrum from the LBNL experiment and Ref. [9] in the K x-ray region is shown in Fig. 3(b). Although six photons were observed within 2σ of expected $K\alpha2$ and $K\beta2$ x-ray energies, assignment of any of these photons as K x rays is complicated by several factors: A level scheme with discrete (non-x-ray) transitions in the K x-ray region can be produced with the available data, and GEANT4 simulations of that level scheme agree well with the experimental data. Furthermore, background from transitions above the K-shell edge are expected to contribute 3.0 Compton events to the K x-ray region, thus a characteristic x-ray spectrum (as defined above) is required. This was not observed: The largest peak in the K x-ray spectrum ($K\alpha1$) is not reproduced in the experimental data, neither of the $K\alpha$ peaks were 2σ above background and the $K\alpha : K\beta$ ratio was 1:1 instead of the expected 3:1. As such, no strong evidence for K x rays due to highly converted $M1$ transitions as suggested in Ref. [9]

was observed, and *Z* identification was not possible with the combined data set.

Forty-six new correlated α-decay chains were observed in the reaction between ^{243}Am and ^{48}Ca, all of which were assigned to formation and decay of ^{288}115. α-photon coincidences observed with the decay steps ^{280}Rg $\rightarrow$ ^{276}Mt and ^{276}Mt $\rightarrow$ ^{272}Bh were used to propose decays schemes for these isotopes. No *K* x rays were definitively identified in this Rapid Communication, and *Z* identification was not possible. GEANT4 simulations of level schemes derived from the experimental data indicate that *Z* identification using the ^{48}Ca + ^{243}Am reaction may well have to wait for the next generation of stable ion-beam facilities. However, this experiment and Ref. [9] have successfully demonstrated that the nuclear structure of SHE daughters can be probed, even with the production of only tens of atoms.

[1] Y. T. Oganessian, J. Phys. G: Nucl. Part. Phys. **34**, R165 (2007).

[2] Y. T. Oganessian *et al.*, Phys. Rev. Lett. **104**, 142502 (2010).

[3] Y. T. Oganessian and V. K. Utyonkov, Rep. Prog. Phys. **78**, 036301 (2015).

[4] L. Stavsetra *et al.*, Phys. Rev. Lett. **103**, 132502 (2009).

[5] P. A. Ellison *et al.*, Phys. Rev. Lett. **105**, 182701 (2010).

[6] C. E. Düllmann *et al.*, Phys. Rev. Lett. **104**, 252701 (2010).

[7] J. M. Gates *et al.*, Phys. Rev. C **83**, 054618 (2011).

[8] S. Hofmann *et al.*, Eur. Phys. J. A **32**, 251 (2007).

[9] D. Rudolph *et al.*, Phys. Rev. Lett. **111**, 112502 (2013).

[10] S. Hofmann *et al.*, Eur. Phys. J. A **48**, 62 (2012).

[11] J. Khuyagbaatar *et al.*, Phys. Rev. Lett. **112**, 172501 (2014).

[12] R. Eichler *et al.*, Radiochim. Acta **98**, 133 (2010).

[13] T. A. Carlson *et al.*, Nucl. Phys. **A135**, 57 (1969).

[14] T. A. Carlson and C. W. Nestor, Jr., At. Data Nucl. Data Tables **19**, 153 (1977).

[15] B. Fricke and G. Soff, At. Data Nucl. Data Tables **19**, 83 (1977).

[16] C. E. Bemis *et al.*, Phys. Rev. Lett. **31**, 647 (1973).

[17] R. D. Herzberg and P. T. Greenlees, Prog. Part. Nucl. Phys. **61**, 674 (2008).

[18] D. Rudolph *et al.*, Acta Phys. Pol., B **45**, 263 (2014).

[19] K. E. Gregorich, Nucl. Instrum. Methods Phys. Res., Sect. A **711**, 47 (2013).

[20] J. F. Ziegler, Nucl. Instrum. Methods Phys. Res., Sect. B **219-220**, 1027 (2004).

[21] G. K. Pang (unpublished).

[22] Y. T. Oganessian *et al.*, Phys. Rev. C **87**, 014302 (2013).

[23] See Supplemental Material at http://link.aps.org/supplemental/10.1103/PhysRevC.92.021301 for a table which provides detailed information on the decay chains presented in this Rapid Communication.

[24] U. Forsberg *et al.*, arXiv:1502.03030.

[25] J. Allison *et al.*, IEEE Trans. Nucl. Sci. **53**, 270 (2006).

[26] S. Agostinelli *et al.*, Nucl. Instrum. Methods Phys. Res., Sect. A **506**, 250 (2003).

[27] T. Kibédi *et al.*, Nucl. Instrum. Methods Phys. Res., Sect. A **589**, 202 (2008).

[28] C. Qi *et al.*, Phys. Rev. C **80**, 044326 (2009).